ChemComm

Dynamic Article Links

Cite this: *Chem. Commun.*, 2012, **48**, 534–536

www.rsc.org/chemcomm

COMMUNICATION

Varying molecular interactions by coverage in supramolecular surface chemistry†‡

Yeliang Wang,[db] Stefano Fabris,[c] Thomas W. White,[a] Federico Pagliuca,[e] Paolo Moras,[f] Marco Papagno,[f] Dinesh Topwal,[g] Polina Sheverdyaeva,[f] Carlo Carbone,[f] Magalí Lingenfelder,§[d] Thomas Classen,¶[d] Klaus Kern[dh] and Giovanni Costantini*[ad]

Received 23rd July 2011, Accepted 3rd October 2011
DOI: 10.1039/c1cc14497a

The possibility of modifying the intermolecular interactions of absorbed benzene-carboxylic acids from coordination to hydrogen bonding by changing their surface coverage is demonstrated through a combination of scanning tunnelling microscopy, X-ray photoemission spectroscopy and density functional theory calculations.

The attention towards surface-supported chemistry has historically been driven by the field of heterogeneous catalysis. More recently, the direct on-surface fabrication of functional nanoarchitectures with potential applications in emerging technologies such as molecular electronics and photovoltaics, (bio)recognition and nanomedicine has strongly invigorated this interest. Supramolecular surface chemistry has become the centre of a research stream aimed at translating essential reaction pathways developed for 3D solution chemistry into 2D equivalents. Many different nanostructures have been fabricated based on assembly strategies involving van der Waals,[1,2] π–π,[3,4] hydrogen bonding,[5,6] metal–organic,[7–9] and, quite recently, also covalent interactions[10–12] (or combinations thereof). Very often the results show strong analogies with the 3D counterparts although, in some cases, the presence of the surface directs the assembly of specific 2D structures. Here we show a noteworthy example of such distinctiveness by demonstrating that the intermolecular interactions of terephthalic acid (TPA) deposited on Cu(110) change from coordination to hydrogen bonding by increasing the molecular coverage. This outcome has no counterpart in solution chemistry and can only be rationalised by taking into account the active role of the substrate.

Samples were prepared under ultrahigh vacuum by evaporating TPA onto a Cu(110) surface held at room temperature, followed by annealing to 450 K. The supramolecular structures analysed in this work develop in the lower coverage regime, *i.e.* before the molecules adopt an upright adsorption geometry.[13] Experimental details of the scanning tunnelling microscopy (STM) and X-ray photoemission spectroscopy (XPS) measurements as well as of the density functional theory (DFT) calculations are reported in the ESI.‡

Three main distinct supramolecular phases were observed by increasing the TPA coverage, σ. Fig. 1a displays a typical STM image of the first one which is observed for $\sigma < 1$ TPA per nm^2. The molecules organise into extended, well-ordered and compact islands which form readily at room temperature and become larger and fewer upon annealing to 450 K. A distinctive characteristic of this phase is the appearance of alternate brighter and dimmer rows along the [001] surface direction. The former consist of 7.2 ± 0.6 Å long elliptical protrusions forming an angle of +50° or −50° (±2°) with respect to [001] and having the same orientation within each row. These protrusions are assigned to individual TPAs since their size is compatible with a flat-lying adsorbed molecule.[7,13–17] The darker rows, denoted by arrows in Fig. 1a, comprise rounded features which, following previous findings,[18–21] are identified as Cu adatoms. This assignment is strongly supported by the DFT calculations presented below. The separation between the TPA or the Cu rows is 12.7 ± 0.2 Å, which corresponds to five Cu lattice spacings along the substrate [1$\bar{1}$0] direction. However, sequential TPA rows are separated by a plane of mirror symmetry, resulting in alternating TPA orientations. This specular symmetry results in a staggering of the Cu protrusions in successive lines and therefore in an effective 10× periodicity along [1$\bar{1}$0]. Within each [001]-row the periodicity is 7.2 ± 0.2 Å, equivalent to two substrate lattice spacings. The supramolecular overlayer of this phase is thus characterised by an overall (10 × 2) periodicity.

By increasing coverage, the (10 × 2) islands become bigger and denser until they occupy the entire substrate, with

[a] *Department of Chemistry, University of Warwick, Gibbet Hill Road, Coventry, CV47AL, UK. E-mail: G.Costantini@Warwick.ac.uk; Tel: +44 24 765 24934*
[b] *Institute of Physics, Chinese Academy of Sciences, 100190 Beijing, P. R. China*
[c] *CNR-IOM DEMOCRITOS, Theory@Elettra Group, Istituto Officina dei Materiali and SISSA, Scuola Internazionale Superiore di Studi Avanzati, via Bonomea 265, I-34136, Trieste, Italy*
[d] *Max-Planck-Institut für Festkörperforschung, Heisenbergstr. 1, D -70569 Stuttgart, Germany*
[e] *Dipartimento di Fisica, Università di Modena e Reggio Emilia, and S3 Center, CNR – Istituto di Nanoscienze, Modena, Italy*
[f] *Istituto di Struttura della Materia, Consiglio Nazionale delle Ricerche, 34149 Trieste, Italy*
[g] *ICTP, Strada Costiera 11, 34151 Trieste, Italy*
[h] *Institut de Physique de la Matière Condensée, Ecole Polytechnique Fédérale de Lausanne, CH-1015 Lausanne, Switzerland*
† This article is part of the ChemComm 'Molecule-based surface chemistry' web themed issue.
‡ Electronic supplementary information (ESI) available. See DOI: 10.1039/c1cc14497a
§ Present Address: Institut de Ciència de Materials de Barcelona, Consejo Superior de Investigaciones Científicas. Campus de la Universitat Autònoma de Barcelona, 08193 Bellaterra, Spain.
¶ Present Address: Robert Bosch GmbH, Germany.

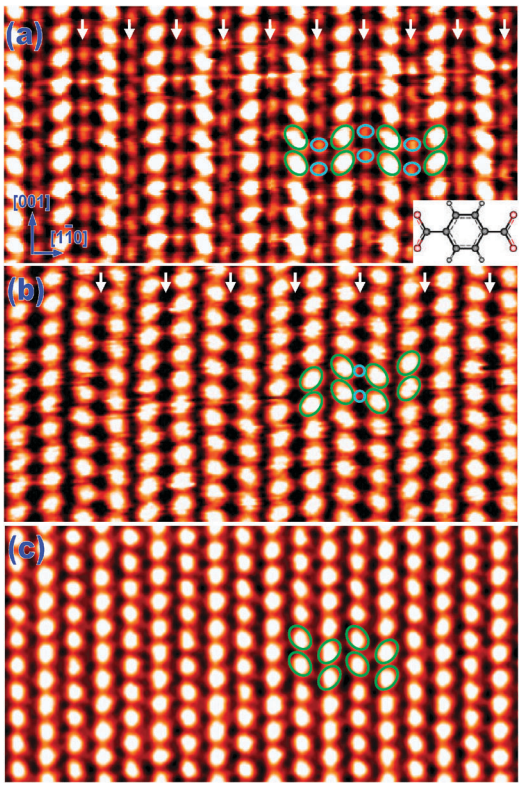

Fig. 1 STM images of TPA adsorbed on Cu(110) at increasing molecular coverage. (a) Phase formed below 1 TPA per nm^2. Arrows denote the position of adatom rows while green and cyan circles indicate TPA molecules and Cu dimers, respectively. The structure of a deprotonated TPA molecule is illustrated in the inset. (b) Phase formed between 1 and 1.5 TPA per nm^2. (c) Phase formed above 1.5 TPA per nm^2. Image size: 14 nm × 7 nm.

$\sigma \approx 1$ TPA per nm^2. Above this threshold, annealing the sample to 450 K leads to a different long-range ordered supramolecular structure (Fig. 1b). This is characterised by pairs of bright [001]-rows composed of $+50^\circ$ and -50° rotated elliptic features which again are identified as individual flat-lying TPA molecules. The molecular double rows are intercalated by darker lines (arrows in Fig. 1b). These present regular shallow protrusions which, as detailed in the following, can also be assigned to Cu adatoms. The distance between successive adatom lines or successive pairs of molecular rows is 17.8 ± 0.3 Å, corresponding to seven Cu lattice spacings along [1$\bar{1}$0]. However, similarly to the lower coverage phase, consecutive Cu adatom lines are staggered and molecules in successive rows are specular symmetric to each other, resulting in an actual 14× periodicity along [1$\bar{1}$0]. The two-fold periodicity along [001] generates a (14 × 2) overall symmetry.

Coverages above 1.5 TPA per nm^2 and annealing at 450 K drive the formation of a third supramolecular arrangement (Fig. 1c). Also this third phase consists of [001]-oriented molecular rows that are very similar to those of the previous phases. However, a distinctive difference here is the absence of any dimmer feature that could correspond to Cu adatoms. All measurable protrusions have the same height and an elliptical shape that identifies them as TPA molecules. Adjacent molecular lines are mutually shifted causing a herringbone arrangement of TPA molecules. A precise measurement reveals that the inter-row separation is 7.7 ± 0.3 Å, corresponding to three times the surface

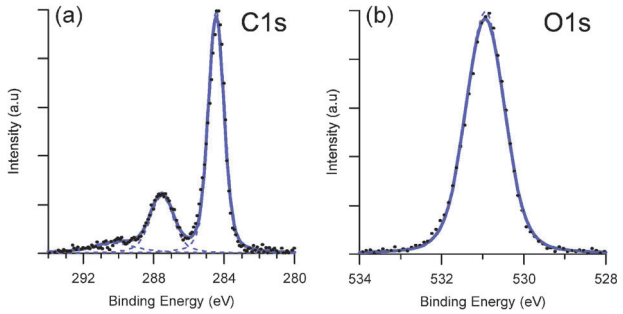

Fig. 2 Representative XPS spectra of the C1s (a) and the O1s (b) core levels in the TPA/Cu(110) system (see ESI‡ for details on the peak fitting procedure).

lattice constant along [1$\bar{1}$0]. The intra-row periodicity is that of the previous phases, *i.e.* twice the substrate lattice along [001]. All molecules within a row have the same $+50^\circ$ or -50° orientation while molecules in neighbouring rows are specular symmetric. As a consequence, the overall superstructure has a (6 × 2) periodicity.

XPS measurements of the C1s and O1s core levels performed on the three phases result in very similar spectra, indicating that the chemical environment of these species does not change appreciably during the phase transitions. Fig. 2a shows a representative spectrum for the carbon signal which is characterised by two main peaks, a larger one centred around 284 eV, related to the six aromatic carbons, and a smaller at 288 eV, due to the remaining two oxygen-bound carbons. The binding energy of the latter is indicative of a carboxylate moiety,[14,21] demonstrating that the TPA molecules are deprotonated in all three supramolecular phases. Supporting this observation is the O1s spectrum (Fig. 2b), which shows a singular narrow peak centred at 531 eV, attributed to the two identical carboxylate oxygens.[14,21,23]

Based on the STM and XPS results, first principle DFT calculations were performed to determine the structure of all three phases. The lowest-energy configuration compatible with the periodicity at lower TPA coverage is displayed in Fig. 3a. This is an ordered metal–organic supramolecular structure exposing dimers of copper adatoms, which coordinatively bind with the carboxylate moieties of two neighbouring terephthalate molecules. According to our DFT calculations, the TPA molecules deprotonate on Cu(110) and adsorb with the aromatic rings parallel to the substrate. Besides the metal–organic bonding along [1$\bar{1}$0], the molecules interact along the [001] direction *via* double hydrogen bonds. The simulated STM image closely agrees with the experimental data, with the Cu dimer imaged as a single round spot and the TPA molecules as brighter elongated protrusions.

Metal–organic bonds also embody the DFT lowest-energy configuration for the successive phase, as illustrated in Fig. 3b. The orientation and bonding of the TPA molecules are very similar to those of the Cu dimer phase, but the higher molecular coverage implies a decrease of the density of Cu adatoms in the supramolecular network. In this intermediate TPA coverage phase, the metal–organic bonding develops at singular Cu adatoms and involves only one carboxylate molecular moiety, while the other binds directly to the substrate. This is reflected in the faint interconnections between TPA double rows displayed by the simulated STM images, in excellent agreement with the measurement. Besides the lower density of Cu adatoms, the local atomic environment is overall very similar to that of

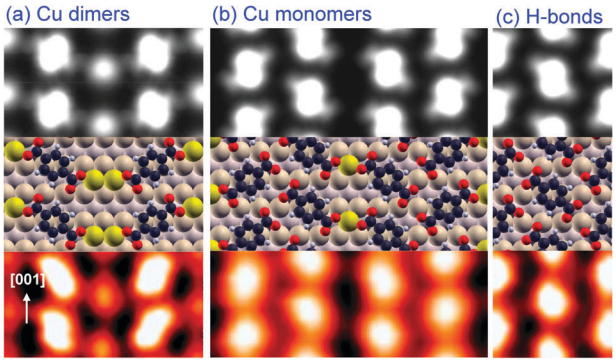

Fig. 3 From top to bottom: DFT simulated STM images, corresponding lowest energy configuration and close-up experimental images for three phases of TPA on Cu(110).

the dimer phase, thus justifying the almost identical XPS spectra of the two systems.

The lowest-energy configuration with a (6 × 2) periodicity predicted by the DFT calculations is displayed in Fig. 3c. This structure does not contain any Cu adatoms and consists exclusively of deprotonated TPA molecules, mutually interacting by hydrogen bonds. The excess Cu adatoms that are excluded from the denser supramolecular structure in both phase transitions most probably condense onto step edges during the substrate annealing.

The calculated free-energy of formation of the three phases can be used to rationalise the coverage-dependent transitions observed in STM. In particular, we consider the formation energy per molecule of each phase with respect to the energy of a deprotonated TPA molecule in vacuum; the contribution of the Cu adatoms is also taken into account by including their formation energy from step edges. The calculated values are −5.8 eV, −5.5 eV and −5.2 eV for the Cu dimer, the Cu monomer and the H-bonded phases, respectively (Fig. 4). This indicates that the dimer phase is the energetically preferred one which agrees with the experimental observation that only this arrangement is formed at $\sigma < 1$ TPA per nm^2. Above this critical coverage σ_I, which reflects the formation of a full monolayer of the Cu dimer phase, additional TPA molecules can either adsorb into a second layer (dot-dashed red line) or reconstruct into a denser single-layer network (Cu monomer phase, full green line). The formation energy per molecule of the Cu monomer phase is higher than that of the dimer phase, but at $\sigma > \sigma_I$ the former can accommodate more TPA molecules hence lowering the overall energy. A similar argument applies for the critical coverage σ_{II}, which separates the Cu monomer from the H-bonded phase.

Since TPA is a model functional molecule, its deposition has been extensively investigated on different substrates. TPA adsorbs in the unmodified acidic form on inert surfaces such as Au(111)[15] while it deprotonates on catalytically active ones like Pd(111).[22] The presence of free metal adatoms, either intentionally co-deposited or thermally released from step edges and kink sites, further catalyses the deprotonation reaction.[19] The resulting highly reactive [COO$^-$] groups bind with the adatoms forming coordination complexes that organise into supramolecular metal–organic structures.[13,14,20,23] This situation is in many respects very similar to what happens in solution chemistry where deprotonation is triggered by pH and the formation of coordination bonds requires the presence of metal

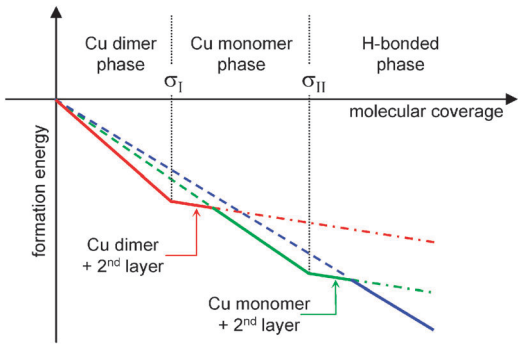

Fig. 4 Schematic diagram of the total formation energy for the TPA/Cu(110) system as a function of molecular coverage. σ_I and σ_{II} are the maximum coverage in the Cu dimer and monomer phases, respectively. Dashed lines represent the energy the system would have if all molecules were in the same phase. Dash-dotted lines are a tentative (not calculated) representation of the energy for second layer molecules. The full line indicates the actual supramolecular configuration adopted by the system.

cations. However, the present study demonstrates that surface chemistry can also exhibit distinctive differences. In fact, since TPA deprotonates upon adsorption onto Cu(110) and the density of free copper adatoms is very high at room temperature,[14,16] the formation of coordination structures should be highly preferential for the TPA/Cu(110) system. Nevertheless, our combined experimental and theoretical analysis reveals that the development of metal–organic complexes critically depends on the molecular surface density and can be completely inhibited at high TPA coverage. Such a scenario has no counterpart in three-dimensional solution chemistry and is a direct consequence of the reactions occurring on a finite two-dimensional support.

We thank N. Lin for fruitful discussion. YLW acknowledges the Humboldt Foundation and NSFC, China. TWW acknowledges a scholarship from the University of Warwick through the URSS scheme. FP is grateful to the Max Planck Society for financial support. We acknowledge the use of the XPSmania software analysis developed by F. Bruno (ALOISA beamline staff, CNR-IOM, Trieste, 2007).

Notes and references

1 P. Sony, *et al.*, *Phys. Rev. Lett.*, 2007, **99**, 176401.
2 W. Chen, *et al.*, *Chem. Commun.*, 2008, 4276–4278.
3 K. Wong *et al.*, *J. Am. Chem. Soc.*, 2004, **126**, 7762–7763.
4 M. Böhringer, *et al.*, *Angew. Chem., Int. Ed.*, 1999, **38**, 821–823.
5 G. Pawin, *et al.*, *Science*, 2006, **313**, 961–962.
6 U. Schlickum, *et al.*, *J. Am. Chem. Soc.*, 2008, **130**, 11778–11782.
7 M. A. Lingenfelder, *et al.*, *Chem.–Eur. J.*, 2004, **10**, 1913–1919.
8 A. Langner, *et al.*, *Proc. Natl. Acad. Sci. U. S. A.*, 2007, **104**, 17927–17930.
9 N. Lin, *et al.*, *Angew. Chem., Int. Ed.*, 2002, **41**, 4779.
10 J. A. Lipton-Duffin, *et al.*, *Small*, 2009, **5**, 592–597.
11 L. Grill, *et al.*, *Nat. Nanotechnol.*, 2007, **2**, 687–691.
12 M. I. Veld, *et al.*, *Chem. Commun.*, 2008, 1536–1538.
13 D. S. Martin, *et al.*, *Phys. Rev. B*, 2002, **66**, 155427.
14 S. Stepanow, *et al.*, *J. Phys. Chem. B*, 2004, **108**, 19392–19397.
15 S. Clair, *et al.*, *J. Phys. Chem. B*, 2004, **108**, 14585–14590.
16 C. C. Perry, *et al.*, *Surf. Sci.*, 1998, **409**, 512–520.
17 Y. L. Wang, *et al.*, *J. Phys. Chem. C*, 2010, **114**, 13020–13025.
18 D. B. Dougherty, *et al.*, *Surf. Sci.*, 2006, **600**, 4484.
19 N. Lin, *et al.*, *Angew. Chem., Int. Ed.*, 2005, **44**, 1488–1491.
20 T. Classen, *et al.*, *Angew. Chem., Int. Ed.*, 2005, **44**, 6142–6145.
21 T. Classen, *et al.*, *J. Phys. Chem. A*, 2007, **111**, 12589–12603.
22 M. E. Canas-Ventura, *et al.*, *J. Chem. Phys.*, 2006, **125**, 184710.
23 S. L. Tait, *et al.*, *J. Am. Chem. Soc.*, 2008, **130**, 2108–2113.

